THE JOURNAL OF PHYSICAL CHEMISTRY Letters

Perspective

pubs.acs.org/JPCL

Thermodynamics and the Intrinsic Stability of Lead Halide Perovskites $CH_3NH_3PbX_3$

Andrea Ciccioli* and Alessandro Latini

Department of Chemistry, Sapienza − University of Rome, Piazzale Aldo Moro 5, 00185 Rome, Italy

ABSTRACT: The role of thermodynamics in assessing the intrinsic instability of the $CH_3NH_3PbX_3$ perovskites (X = Cl,Br,I) is outlined on the basis of the available experimental information. Possible decomposition/degradation pathways driven by the inherent instability of the material are considered. The decomposition to precursors $CH_3NH_3X(s)$ and $PbX_2(s)$ is first analyzed, pointing out the importance of both the enthalpic and the entropic factor, the latter playing a stabilizing role making the stability higher than often asserted. For $CH_3NH_3PbI_3$, the disagreement between the available calorimetric results makes the stability prediction uncertain. Subsequently, the gas-releasing decomposition paths are discussed, with emphasis on the discrepant results presently available, probably reflecting the predominance of thermodynamic or kinetic control. The competition between the formation of $NH_3(g)$ + $CH_3X(g)$, $CH_3NH_2(g)$ + $HX(g)$ or $CH_3NH_3X(g)$ is analyzed, in comparison with the thermal decomposition of methylammonium halides. In view of the scarce and inconclusive thermodynamic studies to-date available, the need for further experimental data is emphasized.

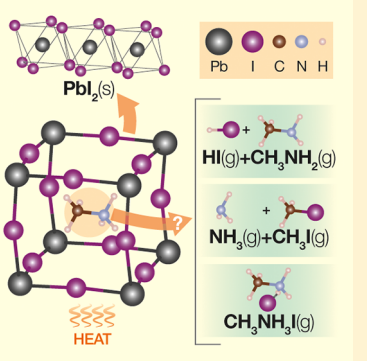

It is no exaggeration to say that the largest part of the current research efforts on lead halide-based and similar perovskite materials is directed toward the search for higher stability needed in photovoltaic applications. In the last five years, many authors expressed the concern that the low stability under the action of a number of external agents, including other device components, could be the main Achilles' heel of this class of light harvester materials, very attractive in other respects, whose prototype is the well-known methylammonium lead iodide, $CH_3NH_3PbI_3$.[1−6] As a consequence, a wealth of strategies were put in place to improve the material and device stability, based on chemical modifications[7−9] protection layers,[10] and encapsulation.[11]

Interaction with water/moisture has been soon identified as a major drawback.[12] Other external agents which many researchers focused on are oxygen and UV/visible radiation.[13] The study of these degradation processes was typically performed by following the change of properties/performances of the material/device, while the interaction takes place or *ex post*. To elucidate the progress and mechanism of degradation, a "microscopic" approach is most often applied, based on techniques such as XRD, UV−vis and NIR spectroscopy, fluorescence, microscopy, XPS, etc.[14−17] Theoretical calculations may be of help in identifying mechanistic details.[18] The effect of temperature on the perovskite stability was usually studied in conjunction with that of such chemical and physical agents. Incidentally, it should be mentioned that in some cases the diagnostic means used to study degradation (e.g., X-ray irradiation, electron currents) can themselves play a role in degradation phenomena.[19,20]

Comparatively little work has been carried out on the intrinsic (in)stability of these materials in itself, both *in vacuo* and under inert atmosphere, as a function of temperature.[21−24] In particular, very few studies are available based on a macroscopic thermodynamic approach.[25−27] Moreover, the available experimental and computational results are often discrepant. The goal of this Perspective is to discuss the issue of the intrinsic stability of $CH_3NH_3PbX_3$ materials from a thermodynamic point of view in light of the information currently available, pointing out the persistent uncertainties and inconsistencies, which make urgent further experimental efforts. Special focus is done on the decomposition processes leading to the release of gaseous products.

Overall, we would like to emphasize in this paper the contribution that classic macroscopic thermodynamics can (or cannot) provide to the stability issues raised from the application of these materials to energy conversion technologies. It is important to underline that the thermodynamic characterization of a material as such is a crucial prerequisite to undertake reliable thermodynamic predictions and simulations of its behavior in various chemical and physical environments. Furthermore, ascertaining the intrinsic (in)stability of a material is essential for practical applications, because if the material is found to be inherently unstable, any protection strategy may be undermined. Regrettably, from an analysis of the literature trends, one has the clear impression that experimental thermodynamic studies cannot keep pace with the wealth of new material modifications that are proposed at an ever-increasing rate to overcome instability issues.

In the broadest sense, investigating the thermodynamic stability of a material means to wonder if, under a given set of external conditions, the material will remain unchanged or it

Received: February 12, 2018
Accepted: June 14, 2018
Published: June 14, 2018

DOI: 10.1021/acs.jpclett.8b00463
J. Phys. Chem. Lett. XXXX, XXX, XXX−XXX

Ascertaining the intrinsic (in)-stability of a material is essential for practical applications, because if the material is found to be inherently unstable, any protection strategy may be undermined.

will undergo some kind of chemical/physical transformation, ultimately driven by entropy production. The number of possible transformation pathways of the system is, in general, high and difficult to predict. In a stricter and more practical sense, one usually evaluates the thermodynamic driving force or affinity, $\Delta_r G = \sum_i \nu_i \mu_i$, for one or a few among the many possible decomposition/degradation reactions, where ν_i and μ_i are, respectively, the stoichiometric coefficients (taken as negative for the left-hand reactants of the chemical/physical degradation process) and the chemical potentials of all the species involved. If the affinity is found to be negative under the conditions of interest (for example, for given pressure and temperature), the selected decomposition/degradation path is thermodynamically favored. Otherwise, the material is stable as far as that path is considered, and indeed its formation from right-hand products is thermodynamically favored. In this approach, the final products of the process are to be known or an hypothesis has to be done. In the case of $CH_3NH_3PbX_3$ compounds, the decomposition to the synthesis precursors was most often considered in theoretical evaluations (Figure 1):

$$CH_3NH_3PbX_3(s) = CH_3NH_3X(s) + PbX2(s) \quad (1)$$

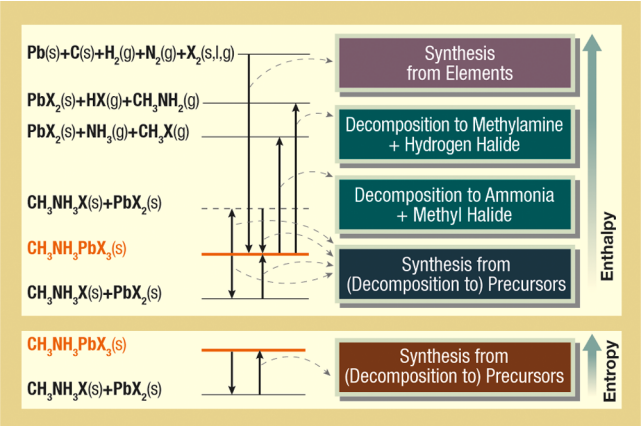

Figure 1. Enthalpy and entropy level scheme for possible formation/decomposition processes of $CH_3NH_3PbX_3$ perovskites. Decomposition to precursors can be both endothermic and exothermic. The minor process leading to the formation of $CH_3NH_3X(g)$ (see Figure 3) is not shown. Enthalpy levels are not to scale.

Although considering this reaction is probably the most natural choice in assessing the formability of $CH_3NH_3PbX_3$ compounds, it should be noted that, while $PbI_2(s)$ was much often reported as the main decomposition product under various conditions, apparently no experimental study reported the CH_3NH_3X solids among the observed products.

A huge number of theoretical calculations were performed to evaluate the energy/enthalpy change of the above reaction by the DFT approach. However, the results are significantly dependent on the chosen functional, the best performance being usually obtained with the PBEsol one, with the additional inclusion of spin−orbit contributions.[28,29] A fairly rich selection of results is reported in Table 1. As for experiments, regrettably, only two direct determinations of $\Delta_r H°(1)$ are available in the literature, both obtained by solution calorimetry at T = 298 K, using DMSO[25] or aqueous HCl[26] as a solvent. Note that, although at 298 K $CH_3NH_3PbI_3$ is stable in the tetragonal form, measurements of ref 25 were performed on the (metastable) cubic high temperature phase. A third experimental value for reaction 1 can be derived from the vapor pressure measurements carried out by effusion-based techniques on the equilibrium (reaction 8) discussed in the next section.[27]

A compilation of all the results is reported in Table 1. Somehow surprisingly, the two calorimetric determinations are not in agreement, showing a discrepancy definitely outside the claimed experimental uncertainties. For $CH_3NH_3PbI_3$, in particular, the very negative value of $\Delta_r H°(1)$ found in ref 26., which led those authors to claim the instability of the compound, was not confirmed by the subsequent measurements in DMSO,[25] making difficult any conclusive prediction on the spontaneous direction of reaction (1) at room temperature for X = I. Also the stability trend from Cl to Br to I is not in agreement between the two studies (Figure 2). The values of ref 26 suggest the Cl > Br > I stability trend, which is consistent with the Goldschmidt's tolerance factor traditionally used to rationalize the stability of perovskite phases. However, tensimetric results[27] agree well with the Ivanov's data,[25] which is a nice occurrence in view of the completely different experimental approach used.

While the enthalpic term is often the most important factor driving the thermodynamic direction of an isothermal chemical

While the enthalpic term is often the most important factor driving the thermodynamic direction of an isothermal chemical reaction, it may well be that the entropic factor comes into play and affects the spontaneity evolution in a decisive manner.

reaction, it may well be that the entropic factor comes into play and affects the spontaneity evolution in a decisive manner. This is especially true for reactions involving gaseous phases, aggregation/disaggregation processes, high temperatures, and when enthalpic effects are small, which is the case of reactions (1). Regrettably, in the last few decades the number of papers presenting heat capacity and absolute entropy measurements is decreasing, making thermodynamic evaluations more difficult and less accurate. It is thus a really lucky occurrence that almost 30 years ago, when lead halide perovskites were far from bursting on the scientific scene, Suga and co-workers published low temperature heat capacity data for the $CH_3NH_3PbX_3$ crystal phases.[41] Absolute entropies of the other compounds involved in reaction 1 are known with the exception of CH_3NH_3Br, whose entropy was estimated by us by the empirical Volume-Based-Thermodynamic approach.[42]

DOI: 10.1021/acs.jpclett.8b00463
J. Phys. Chem. Lett. XXXX, XXX, XXX−XXX

Table 1. Energetic and Thermodynamic Properties of the Decomposition Reactions of $CH_3NH_3PbX_3$ Perovskites to Solid Precursors: $CH_3NH_3PbX_3(s) = CH_3NH_3X(s) + PbX_2(s)$[a]

	theory (DFT)		thermodynamic experiments					
X	ΔE[b]	ref.	ΔH°_{298K}	method and ref	S°_{298K}[c]	ΔS°_{298K}[d]	ΔG°_{298K}	stable with respect to precursors at 298 K, 1 bar[e]
Cl (cubic)	12	30	9.03 ± 1.68	solution calorim. in HCl[26]	313.37	- 38.77	11.6	YES
	68	31	4.45 ± 0.34	solution calorim. in DMSO[25]			16.0	YES
	0.39−3.9	32	2.8 ± 7.8	vapor pressure (KEML, KEMS)[27]			11.6	YES
Br (cubic)	12	30	−6.69 ± 1.41	solution calorim. in HCl[26]	349.29	- 39.9	5.2	YES
	24	31	6.78 ± 0.97	solution calorim. in DMSO[25]			18.7	YES
	1.4−4.1	32	3.3 ± 8.7	vapor pressure (KEML, KEMS)[27]			15.2	YES
I (tetragonal)	2.7−3.4	22		solution calorim. in HCl[26]	374.15	−39.6	−22.7	NO
	9.6	33	- 34.50 ± 1.01					
	2.2	29						
	4.8	34						
	−8.7	35	- 1.913 ± 1.12[f]	solution calorim. in DMSO[25]			9.9	YES
	5.8	36						
	9.6	31						
	−5.8/−6.1	32						
	0.39	37	0.39 ± 9.7	vapor pressure (KEML, KEMS)[27]			11.4	YES
	2.4	38						
	3.9	39						
I (cubic)[g]	−4.8	28	−4.493 ± 1.12	solution calorim. in DMSO[25]	383.85[c]	−49.3	10.2	YES
	−1.9	30						
	26	40						
	−11/−12	32						

[a]Energies and enthalpies are in kJ/mol, entropies in J/K mol. [b]For an accurate comparison of the theoretical ΔEs with the thermochemical ΔH°_{298K}, small effects due to zero-point energy, finite temperature and standard pressure should be considered. The corrections due to the heat content difference ($H_{298\ K}-H_{0K}$) and the $P^\circ\Delta V$ terms are of the order of few kJ/mol and J/mol, respectively. [c]Absolute entropies of $CH_3NH_3PbX_3$ are from ref 41. The value for the high temperature cubic phase of $CH_3NH_3PbI_3$ was estimated by adding the tetragonal-cubic transition entropy (9.7 J/K mol, measured at 330 K[41]) to S°_{298K} of the tetragonal phase. [d]Entropies of $CH_3NH_3X(s)$ and $PbX_2(s)$ are from the compilation of ref 25. except for CH_3NH_3Br, whose $S^\circ_{298K}$was estimated by us as 148.2 J/K mol by a volume-based-thermodynamics approach.[42] [e]Based on the sign of ΔG°_{298K}, which for reactions (1) corresponds to the driving force Δ_rG at 298 K and 1 bar. [f]Evaluated by adding the t-c transition enthalpy (2.58 kJ/mol, measured at 330 K[41]) to the ΔH°_{298K} value measured for the cubic phase.[25] [g]The tetragonal to cubic transition enthalpy of $CH_3NH_3PbI_3$ is 2.58 kJ/mol, measured at 330 K.[41]

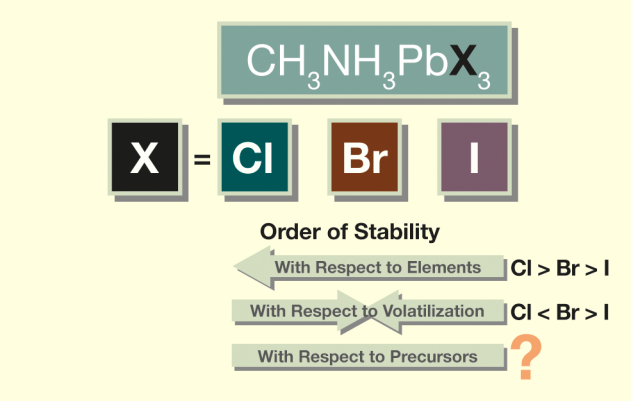

Figure 2. Stability order of $CH_3NH_3PbX_3$ for X = Cl,Br,I with respect to different processes.

The so-derived entropy changes $\Delta_rS^\circ(1)$ at 298 K, also reported in Table 1, are significantly negative (Figure 1) and therefore give a large positive contribution to the decomposition Gibbs energy change, in most cases larger than the enthalpic term, so stabilizing the perovskite phases with respect to precursors. Furthermore, since $\left(\frac{\partial \Delta_rG^\circ}{\partial T}\right)_{P=P^\circ} = -\Delta_rS^\circ$, negative entropy changes cause Δ_rG° of reaction 1 to increase with T, and the decomposition to become more and more disfavored with increasing temperature. It is interesting to note that the largely negative $\Delta_rS^\circ(1)$ values are related to the high absolute entropies of the $CH_3NH_3PbX_3$ phases, in turn due to the high entropy changes associated with the phase transitions in the crystal.

Since reaction 1 involves pure solid phases, Δ_rG° is practically coincident with the thermodynamic driving force for decomposition, Δ_rG, provided that pressure is not too high. The last column of Table 1 indicates the stability of perovskite compounds with respect to precursors of reaction 1. On the basis of the available information, it is concluded that for X = Cl and Br decomposition is thermodynamically disfavored at 298 K, whereas for X = I the results are conflicting: depending on the selected enthalpy change, the negative entropic term can compensate it or not. On the basis of the agreement with tensimetric values, it seems reasonable to recommend provisionally the calorimetric results of Ivanov et al.,[25] which provide the following expressions for the Δ_rG° of decomposition reaction 1:

$$\Delta_rG^\circ(CH_3NH_3PbCl_3)\ (1) = (4.45 + 38.7710^{-3}T)\ \text{kJ/mol} \quad (2)$$

$$\Delta_rG^\circ(CH_3NH_3PbBr_3)\ (1) = (6.78 + 39.9010^{-3}T)\ \text{kJ/mol} \quad (3)$$

DOI: 10.1021/acs.jpclett.8b00463
J. Phys. Chem. Lett. XXXX, XXX, XXX−XXX

$$\Delta_r G^\circ(CH_3NH_3PbI_3)\ (1) = (-1.91 + 39.6010^{-3}T)\ \text{kJ/mol} \quad (4)$$

valid for the room temperature phases (cubic phase for $CH_3NH_3PbCl_3$ and $CH_3NH_3PbBr_3$ and tetragonal for $CH_3NH_3PbI_3$) in a reasonably large temperature range (the temperature dependence of $\Delta_r H^\circ$ and $\Delta_r S^\circ$ is not accounted for in the above equations), including temperatures of practical interest for photovoltaic devices (typically in the range 30−80 °C). According to these expressions, the pervoskite phases are stable at room temperature, and their stability increases at higher temperature. In principle, by putting $\Delta_r G$ equal to zero, the lowest temperature at which the perovskite phases are stable can be roughly estimated. These temperatures correspond to the invariant temperatures (at $P = P^\circ$) where perovskites would coexist in equilibrium with their precursors. Simple linear extrapolation of eqs 2−4 gives temperatures extremely low or even negative, indicating that no decomposition occurs in practice (obviously, both $CH_3NH_3PbX_3$ and the decomposition products would undergo transitions to the low-temperature phases at the corresponding transition temperatures). It is then clear from this analysis, that perovskite phases are "high temperature compounds" in the pseudobinary PbX_2-CH_3NH_3X phase diagram, and reaction 1 should not be regarded as a "thermal" decompositions at all. However, if the $\Delta_r H^\circ$ value of ref 26 is used for the iodide phase, a minimum temperature of stability of 870 K is estimated by rough extrapolation (even higher than the melting point of PbI_2), meaning that the material is completely unsuitable for photovoltaic applications (unless strong kinetic hindrance comes into play).

As mentioned, ascertaining the stability of a material referring to only one or several processes is not a conclusive proof of its absolute intrinsic stability. For example, in order to identify the most favored among a number of possible decomposition pathways of $CH_3NH_3PbI_3$, a convex hull approach was used, leading to select the decomposition to $NH_4I + PbI_2 + CH_2$ as the most stable path.[43] In this connection, it is interesting to note that the cleavage of the C−N bond with formation of hydrocarbon fragments $-CH_2-$ was recently observed in *in situ*-deposited $CH_3NH_3PbI_3$ films by near ambient pressure XPS.[44]

Another process that is sometimes taken as representative of the intrinsic stability of a material is the opposite of the formation from elements, $Pb + 1.5\ X_2 + 3\ H_2 + 0.5\ N_2 + C = CH_3NH_3PbX_3$, with all species in their reference phase (at the temperature of interest) and in the standard state (see Figure 1).[45] Consistent with eqs 2−4, the following expressions can be derived for $\Delta_f G^\circ$ of the $CH_3NH_3PbX_3$ compounds, valid for the room temperature phases in a reasonably large temperature range:

$$\Delta_f G^\circ(CH_3NH_3PbCl_3) = (-662.2 + 579.110^{-3}T)\ \text{kJ/mol} \quad (5)$$

$$\Delta_f G^\circ(CH_3NH_3PbBr_3) = (-543.1 + 437.010^{-3}T)\ \text{kJ/mol} \quad (6)$$

$$\Delta_f G^\circ(CH_3NH_3PbI_3) = (-371.6 + 358.110^{-3}T)\ \text{kJ/mol} \quad (7)$$

These equations indicate that $\Delta_f G^\circ$ is strongly negative at temperatures close to room temperature and show the expected trend of stability with respect to elements, Cl > Br > I (Figure 2). Equations 5−7 can be combined with the corresponding expressions for other substances (H_2O, PbO, $PbCO_3$, HI, CH_3NH_2, etc.) to estimate the standard Gibbs energy change of chemical reactions potentially involved in the intrinsic or extrinsic (e.g., due to water or oxygen) degradation of the materials as well in synthesis and annealing processes. Note that for several important reactions (for example, those forming perovskite hydrate phases such as $(CH_3NH_3)_4PbI_6 \cdot 2H_2O$ under exposure to moisture) $\Delta_r G^\circ$ cannot be evaluated owing to the lack of relevant thermodynamic data.

In view of the above discussion, the decomposition processes (1) should not be a worrisome decomposition path as far as methylammonium lead chloride and bromide perovskites are concerned, whereas the discrepancy between calorimetric data makes a conclusive assessment for iodide difficult. However, other decomposition channels could be at work under operative conditions. In particular, gas-releasing decomposition processes are of crucial importance for investigating the stability of $CH_3NH_3PbX_3$ and similar materials. Grazing-incidence wide-angle X-ray diffraction measurements have shown recently[46] that the dramatic heat-induced performance decrease of encapsulated perovskite-based devices is due to surface modifications related to the intercalation of thermally decomposed methylammonium fragments into PbI_2 planes. Since encapsulation is expected to prevent interaction with external agents, this is a clear evidence of intrinsically driven degradation related to the loss of volatile fragments, as already suggested in previous papers.[22,24] Furthermore, the type of gas that these materials tend to lose under heating may be of interest for real devices because gaseous products could interact with the sealing materials and with the other components of the cell. Finally, gas-phase releasing degradation is very important under conditions where the system is allowed to vaporize, such as postsynthesis annealing[47] and synthesis by vapor deposition techniques.[48] In spite of this, the direct experimental study of the released gaseous species has been the subject of relatively few studies that, unfortunately, presented problematic results.[27,49,50]

In this connection, the following gas-releasing processes are worth considering:

$$CH_3NH_3PbX_3(s) = PbX_2(s) + HX(g) + CH_3NH_2(g) \quad (8)$$

$$CH_3NH_3PbX_3(s) = PbX_2(s) + CH_3X(g) + NH_3(g) \quad (9)$$

$$CH_3NH_3PbX_3(s) = PbX_2(s) + CH_3NH_3X(g) \quad (10)$$

In all three cases, solid lead dihalide is formed, as invariably observed by means of solid state techniques,[27] and the CH_3NH_3X portion of the perovskite phase is lost, either as undissociated methylammonium halide or in the form of smaller molecules. In principle, gas-phase dissociation can occur by formation of HX or CH_3X, depending on whether the methyl group or the proton associates with the halide ion. Theoretical analyses indicate as an energetically favored path to this kind of degradation the creation of HI vacancies and the subsequent combination of the amine fragment with Pb atoms, which disintegrates the inorganic framework.[51]

That the heat-induced degradation of $CH_3NH_3PbI_3$ perovskites proceeds through mass loss has been shown by a number of thermogravimetric (TGA) measurements and has been also inferred by solid state techniques, for example by measuring

DOI: 10.1021/acs.jpclett.8b00463
J. Phys. Chem. Lett. XXXX, XXX, XXX−XXX

the evolution of I/Pb and N/Pb ratios by photoelectron spectroscopy.[20]

Most investigations of the degradation of $CH_3NH_3PbX_3$ to volatile species were carried out by classic TGA, where the mass loss rate is recorded as a function of temperature, usually under an inert dynamic atmosphere. A number of early TGA measurements[23,52−54] led to the conclusion that thermal decomposition of $CH_3NH_3PbX_3$ compounds begins at rather high temperature, above 200−250 °C, giving support to the view that the intrinsic thermal stability was not a major drawback in real applications where temperature does not exceed 80−90 °C. Various authors also showed that mass loss starts at lower temperatures for chloride and mixed iodide−chloride compounds compared to bromide and iodide.[26,54] In the same years some papers based on XRD and other solid-state techniques were less optimiztic[22,55] pointing out that also at temperatures as low as 85−100 °C appreciable decomposition occurred even under an inert atmosphere, especially under prolonged heating. Actually, the dynamic nature of TGA experiments, especially if the used scan rate is not very low, could be insufficient for assessing the long-term stability of a photovoltaic material, which is required to work for a long time at temperatures lower than the decomposition temperatures detectable by TGA curves. Furthermore, the TGA method does not permit distinguishing among processes 8−10, and the attribution of the chemical nature of the gaseous phase has been basically speculative or indirect in the literature, with reaction 8 generally preferred on the basis of chemical wisdom (acid−base interaction between the organic cation and the halide anion). Two-step TGA curves observed by some authors for $CH_3NH_3PbI_3$ suggested the sequential loss of HI(g) and CH_3NH_2(g),[23] supporting this hypothesis.

Most investigations of the degradation of $CH_3NH_3PbX_3$ to volatile species were carried out by classic TGA, where the mass loss rate is recorded as a function of temperature, usually under an inert dynamic atmosphere

To the best of our knowledge, the first reports on the direct detection of the gas phase released by the $CH_3NH_3PbX_3$ perovskites appeared in 2016,[27,49,54] although FTIR spectroscopy experiments were previously reported for the vaporization of dimethylformamide-$CH_3NH_3PbCl_xI_{3-x}$ solutions.[56]

Extensive vaporization experiments were first reported based on the classic Knudsen Effusion Mass Loss (KEML) and Knudsen Effusion Mass Spectrometry (KEMS) techniques.[27] KEMS measurements were carried out on all three $CH_3NH_3PbX_3$ compounds in the overall temperature range 76−144 °C, much lower than decomposition temperatures found in TGA measurements. Mass spectra showed the large dominance of peaks attributable to HX(g) and CH_3NH_2(g), providing strong evidence of the occurrence of reaction 8 previously proposed in ref 54 based on Temperature-Programmed Desorption experiments. Weakest peaks corresponding to undissociated CH_3NH_3X(g) were also detected (it should be pointed out that electron impact mass spectrometry could cause the undissociated CH_3NH_3X(g) species to break into smaller fragment ions.). The thermodynamic analysis of partial pressure data allowed decomposition enthalpies to be derived for reaction 8 and, thereafter, formation enthalpies of $CH_3NH_3PbX_3$ perovskites to also be evaluated. The latter were subsequently found to agree well with calorimetric results (see Table 1).[25,50] Shortly after, another study[49] was published where a very different behavior was observed by TGA-Mass Spectrometry experiments for $CH_3NH_3PbI_3$ and for its precursor halide, CH_3NH_3I, which were found to release only NH_3(g) and CH_3I(g). Although the largest part of TGA-MS experiments were carried out at much higher temperatures (300−420 °C) than Knudsen measurements, authors obtained some indication that the same process would also take place at temperatures as low as 80 °C, close to those of interest for photovoltaic applications. Interestingly, the findings of ref 49 confirmed in part those previously obtained by FTIR.[56] FTIR spectra of the gas phase recorded at 265 °C indicated the decomposition of solid CH_3NH_3I to NH_3(g) and CH_3I(g), in contrast with CH_3NH_3Cl and $CH_3NH_3PbCl_3$, which was observed to release HCl(g) and CH_3NH_2(g).

In order to shed some light on this scanty and discrepant experimental information, a thermodynamic analysis is useful.

In principle, reactions 8−10 may occur simultaneously, giving a three-phase monovariant equilibrium with seven components, two of them thermodynamically independent. While the absolute values of the partial pressures depend on the properties of the two condensed phases, the thermodynamic competition between the three reactions is basically due to the different stability of the gaseous species.

Using relations 5−7 for the Gibbs energy of formation of the perovskite phases and the corresponding well-established expressions for the products of reactions 8 and 9, the results reported in Table 2 are derived for the corresponding standard Gibbs energy changes. Data in Table 2 indicate that, at variance with the trend of formation enthalpies, bromide is the most stable with respect to vaporization decomposition (Figure 2) for both processes 8 and 9. However, the stability trend is Br > I > Cl and Br > Cl > I, respectively, for the two processes. Note that only in the case of reaction 8 is the stability order in agreement with TGA experiments (see above). For the sake of comparison, in the same table, the $\Delta_rG°$'s are also reported for the corresponding decomposition reactions of methylammonium halides, CH_3NH_3X. It is interesting to note that $\Delta_rG°$ values for the latter are lower (i.e., the decomposition pressures are higher for a given temperature) than those of the corresponding perovskites. A

Table 2. Standard Gibbs Energy Changes ($\Delta_rG°$, in kJ/mol) for the Decomposition Reactions of $CH_3NH_3PbX_3$ and CH_3NH_3X with Release of Gaseous Products[a]

X	$CH_3NH_3PbX_3(s) = PbX_2(s) + HX(g) + CH_3NH_2(g)$ (8)	$CH_3NH_3PbX_3(s) = PbX_2(s) + CH_3X(g) + NH_3(g)$ (9)
Cl	$187.9 - 252.3 \times 10^{-3}\ T$	$174.9 - 249.6 \times 10^{-3}\ T$
Br	$206.9 - 253.3 \times 10^{-3}\ T$	$183.3 - 250.3 \times 10^{-3}\ T$
I[b]	$200.2 - 250.1 \times 10^{-3}\ T$	$164.7 - 247.2 \times 10^{-3}\ T$
	$CH_3NH_3X(s) = HX(g) + CH_3NH_2(g)$	$CH_3NH_3X(s) = CH_3X(g) + NH_3(g)$
Cl	$183.5 - 291.1 \times 10^{-3}\ T$	$170.5 - 288.3 \times 10^{-3}\ T$
Br	$200.1 - 293.3 \times 10^{-3}\ T$	$176.6 - 290.3 \times 10^{-3}\ T$
I	$204.7 - 289.7 \times 10^{-3}\ T$	$169.2 - 286.8 \times 10^{-3}\ T$

[a]These expressions can be applied in a reasonably large temperature range near to 298 K. [b]Cubic phase of $CH_3NH_3PbI_3$.

DOI: 10.1021/acs.jpclett.8b00463
J. Phys. Chem. Lett. XXXX, XXX, XXX−XXX

large part of this effect is due to the higher entropy changes for the decomposition of CH_3NH_3X compounds.

A similar analysis for process 10 is made difficult by the lack of thermodynamic data for the species $CH_3NH_3X(g)$, which is not surprising if we consider that, even for the simpler ammonium halide species, $NH_4X(g)$, experimental data are more uncertain than one might believe. For example, the dissociation degree of $NH_4Cl(g)$ to $NH_3(g)$ and HCl(g) has been the subject of a longstanding debate, with experimental results ranging from complete to very limited dissociation and theoretical studies claiming for a fair stability of the undissociated hydrogen-bond linked species.[57] Although the CH_3NH_2 + HCl potential energy surface has been the subject of a number of theoretical studies aimed at clarifying the mechanism of the methyl exchange in solution phase (the so-called Menshutkin S_N2 reaction, $CH_3Cl + NH_3 = CH_3NH_3^+Cl^-$), apparently a stable structure for the CH_3NH_3Cl complex in the gas phase was reported only recently by Patterson[58] based on DFT calculations. In order to evaluate the relative importance of reaction 10 for the iodide perovskite under thermodynamic conditions, similar calculations were done for the $CH_3NH_3I(g)$ species,[59] that allowed us to derive an approximate estimate of $\Delta_rG°(10)$ as

$$\Delta_rG°(10) = (143.8 - 111.310 - 3T)\ \text{kJ/mol} \quad (X = I) \tag{11}$$

(cubic phase of $CH_3NH_3PbI_3$). From the equations in Table 2 and eq 11, the partial pressures of all the gaseous species in equilibrium with $CH_3NH_3PbI_3$ and PbI_2 were estimated. The so-derived *total* pressures produced from reactions 8−10 are reported in Figure 3 along with the total pressures measured by the classic Knudsen effusion method[27,60] (the only experimental value available to date). This plot shows clearly that, under the hypothesis of thermodynamic equilibrium, the decomposition channel of $CH_3NH_3PbI_3$ leading to NH_3 + CH_3I (process 9) should be by far the most important, especially at moderate temperatures, followed by that one releasing CH_3NH_2 + HI and eventually by the evaporation to the undissociated species, which is negligible at any temperature of interest. However, the decomposition pressure due to the loss of NH_3 + CH_3I should be 2−3 orders of magnitude higher than that experimentally observed under effusion conditions, which instead agrees well with the occurrence of process 8. It should be pointed out that our thermodynamic prediction is entirely based on calorimetric results (eqs 5−7). Being such data are completely independent from tensimetric measurements, the agreement with the latter is very satisfactory. It should also be pointed out that our calculation for process 10 is based on computationally estimated thermodynamic data.

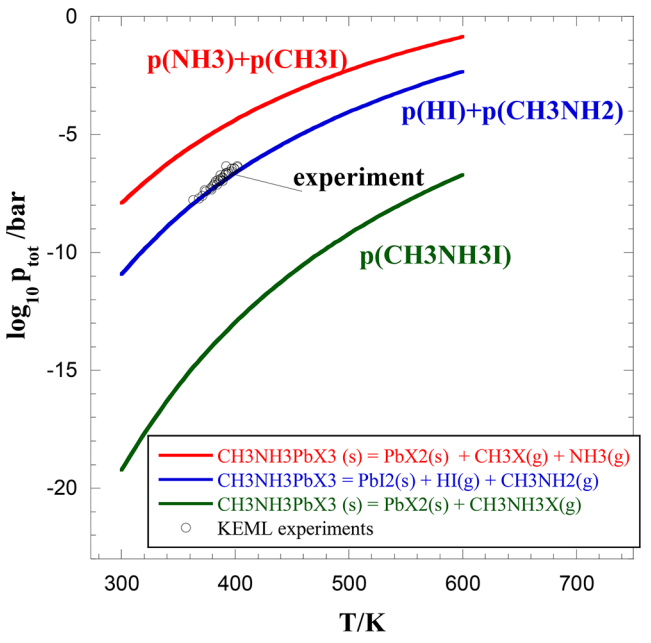

Figure 3. Total pressures produced by decomposition processes 8−10 evaluated from calorimetric data, compared to the results of KEML experiments.[27,60]

Overall, from this analysis the conclusion can be drawn that (*i*) process 9 has a much larger thermodynamic driving force, but (*ii*) under effusion conditions, which, in principle, should allow an approach toward thermodynamic equilibrium, the occurrence of this process is kinetically hindered, and the measured pressures suggests that process 8 takes place instead. The kinetic limitation of reactions 9 seems quite plausible because the breaking of a strong C−N bond (330 kJ/mol at 298 K) is required, instead of the hydrogen-bond breaking involved in process 8. This view is supported by DFT calculations,[49] which predict a remarkable activation barrier for reaction 9, and by the comparison with the thermal decomposition behavior of simple alkylammonium halides (see below). It should be noted that the very good agreement between calculated and experimental data indicates that, as far as process 8 is concerned, thermodynamic equilibrium is fully attained under Knudsen conditions, giving confidence in the thermodynamic properties derived from tensimetric measurements, provided that data are analyzed on the basis of the proper reaction.

In view of the above analysis, the aforementioned experimental results on the decomposition of $CH_3NH_3PbX_3$ (especially in regard to $CH_3NH_3PbI_3$) are somehow puzzling. Apparently, measurements under Knudsen conditions, which are supposed to favor the attainment of thermodynamic equilibrium, gave evidence for the occurrence of the thermodynamically disfavored process 8, whereas "open-pan" TGA-MS and IR experiments provided evidence for the occurrence of the thermodynamic pathway. Since the latter experiments were mostly performed in a much higher temperature range where kinetic hindrance might be overcome, the question arises whether different temperatures alone can account for the experimental findings or other effects are to be invoked, such as vacuum versus dynamic inert atmosphere, heating scan versus thermal equilibration, presence of a heated transfer line, etc.

More recent KEMS experiments[50] where the competition between processes 8 and 9 was studied by measuring the $p(HI)/p(CH_3I)$ ratio under different conditions, provided some additional information. The competition between the two processes is basically driven by the following homogeneous pressure-independent gaseous equilibrium:[50]

$$HX(g) + CH_3NH_2(g) = CH_3X(g) + NH_3(g) \tag{12}$$

Since the gaseous species come in 1:1 molar ratio from the $CH_3NH_3PbX_3$ solid, at equilibrium $p(HX) = p(CH_3NH_2) \equiv p(8)$ and $p(CH_3X) = p(NH_3) \equiv p(9)$, with

DOI: 10.1021/acs.jpclett.8b00463
J. Phys. Chem. Lett. XXXX, XXX, XXX−XXX

$$\frac{p(8)}{p(9)} = \exp\left(\frac{\Delta_r G^\circ(12)}{2RT}\right) \quad (13)$$

In view of the small entropy change of reaction 12, the partial pressure ratio 13 is ruled by the enthalpic factor. Since ammonia is much more thermally stable than methylamine ($\Delta_f H^\circ_{298}$ = −45.94 and −22.5 kJ/mol, respectively), at the temperatures of interest equilibrium 12 is shifted toward the right, regardless of the nature of X. Furthermore, since HI is thermally unstable ($\Delta_f H^\circ_{298}$ = +26.5 kJ/mol) compared to CH_3I ($\Delta_f H^\circ_{298}$ = 14.4 kJ/mol), the decomposition channel 8 is especially disfavored for iodide. The reverse holds for chloride ($\Delta_f H^\circ_{298}$ = −92.3 and −81.9 kJ/mol for HCl and CH_3Cl, respectively), whereas the thermal stabilities of CH_3Br and HBr are practically equal ($\Delta_f H^\circ_{298}$ = −36.3 and −36.4 kJ/mol). Being exothermal, reaction 12 tends to shift to left at higher temperatures, although right-hand products remain strongly favored at any temperature of interest. In Figure 4, the p(HI)/p(CH_3I) pressure ratio calculated by eq 13 is reported, along with the corresponding ratios measured by KEMS in a higher temperature range compared to ref 27, using two different effusion caps.[50] The red line refers to experiment carried out with an ordinary effusion hole (1 mm diameter, negligible thickness), the blue one was derived using a sort of "chimney" orifice, with 0.5 mm in diameter and a 6.5 mm long channel making the effusion rate lower (see the cap pictures in Figure 4). The higher impedance to effusion flow is expected to favor approaching the heterogeneous equilibrium. Indeed, Figure 4 clearly shows that (*i*) higher temperatures do favor the formation of CH_3I (g) versus HI(g), contrarily to thermodynamic predictions (black line with negative slope in Figure 4), and (*ii*) high impedance effusion conditions have the same effect, decreasing the HI/CH_3I ratio by more than 1 order of magnitude. A schematic picture of these findings is reported in Figure 5. Nevertheless, under all the explored conditions, process 8 remains the dominant decomposition pathway. Therefore, according to KEMS results, even at temperature as high as 250 °C, process 9 cannot come out by the extent predicted by equilibrium thermodynamics.

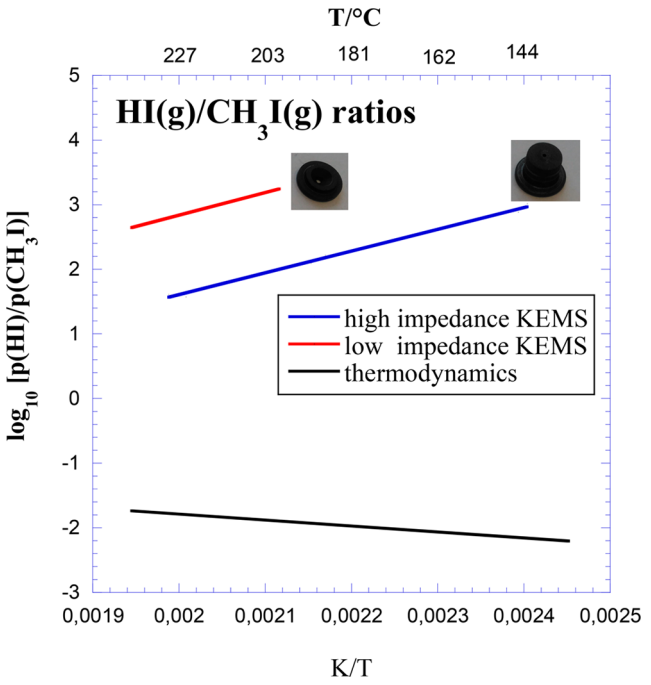

Figure 4. HI(g)/CH_3I(g) partial pressures ratios illustrating the competition between the decomposition processes 8 and 9. Red and blue lines refer to KEMS measurements performed, respectively, with low flow impedance (ordinary effusion cap) and high flow impedance (chimney-like cap).[50]

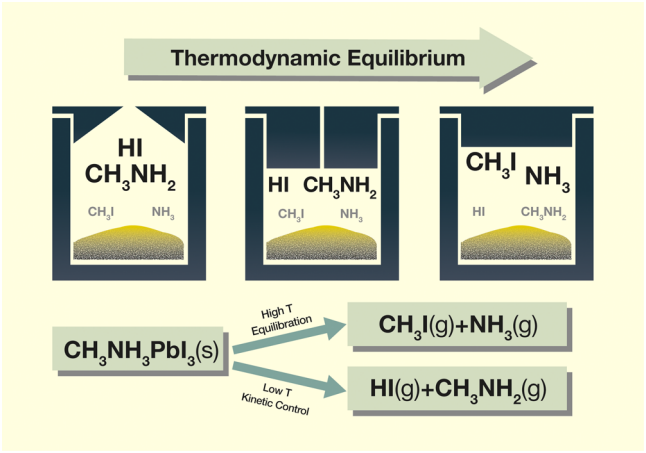

Figure 5. Graphic representation of the experimental conditions leading to kinetically controlled (process 8) or thermodynamically controlled (process 9) decomposition pathways. Higher temperatures and/or closer-to-equilibrium conditions favor the thermodynamic control.[50]

In an attempt to rationalize the observed decomposition behavior of $CH_3NH_3PbX_3$ perovskites, a possible benchmark is given by the thermal decomposition of simple mono- di-, tri-, and tetraalkylammonium halides, which have been the subject of quite a high number of studies.[61−63] On the basis of TGA experiments, Błażejowski and co-workers concluded that compounds of general formula $R_pNH_{4-p}X$ decompose under heating according to the following processes:[62]

$$R_pNH_{4-p}X(s) = R_pNH_{3-p}(g) + HX(g) \quad p = 1,2,3 \quad (14)$$

$$R_pNH_{4-p}X(s) = R_{p-1}N(g) + RX(g) \quad p = 4 \quad (15)$$

In other words, mono-, di- and trialkyl ammonium halides decompose, releasing the corresponding amine and hydrogen halide rather than by the alternative process releasing the alkyl halide and the less substituted amine:

$$R_pNH_{4-p}X(s) = R_{p-1}NH_{4-p}(g) + RX(g) \quad (16)$$

whereas tetralkylammonium halides, which do not contain hydrogen atoms, decompose by loss of alkyl halide and trialkylamine. The occurrence of the latter process was also confirmed by direct FTIR spectroscopy experiments.[63]

As far as thermodynamic equilibrium is concerned, the above-reported discussion on the competition between processes 8 and 9 could be extended to processes 14 and 16. Actually, the pressure ratio (process 12) in equilibrium with the $CH_3NH_3PbX_3$ + PbX_2 mixture is the same as that in equilibrium with the methylammonium halide solids CH_3NH_3X, and it is ruled by the relative stability of NH_3(g) versus CH_3NH_2(g) and HX(g) versus CH_3X(g), which would strongly favor process 16 (see above). Other cases can be more complex, since the relative stability of HX(g) and RX(g)

DOI: 10.1021/acs.jpclett.8b00463
J. Phys. Chem. Lett. XXXX, XXX, XXX−XXX

depends markedly on X and that of $R_pNH_{3-p}(g)$ versus $R_{p-1}NH_{4-p}(g)$ for p = 2,3 is not obvious.

The kinetic hindrance of the C−N bond-breaking process involved in decomposition reactions 15 and 16 is supported by the fact that quaternary amines, where process 14 cannot take place, are observed to decompose at much higher temperatures than less substituted compounds.[63] Furthermore, the enthalpy changes of the thermal decomposition of tetralkylammonium halides as measured by TGA have been found to be much higher than those measured by DSC (for instance, 319.7 kJ/mol versus 186.7 kJ/mol for $(CH_3)_4NI$[63]), which correspond to the actual energy required to convert the solid into gaseous products (i.e., the thermodynamic decomposition enthalpy). In TGA measurements, where the enthalpy change is obtained by the temperature dependence of the mass loss rate, the activation barrier is instead measured. DFT calculations fully support this view. For example, an activation energy of 239 kJ/mol was calculated recently[64] for the thermodynamically favored decomposition of dioctylammonium chloride to dioctylamine +1-chlorooctane, whereas no activation barrier is found for the alternative process leading to trioctylammonium chloride and HCl. While the outlined frame of the thermal behavior of alkylammonium halide seems fairly well-established, nonetheless the direct experimental evidence of process 14 for mono-, di-, and trisubstituted compounds seems scarce, and indeed recent perovskite-related experiments seem to call it into question.[49,56]

In conclusion, the intrinsic stability of $CH_3NH_3PbX_3$ perovskites can be analyzed in the light of a classical thermodynamic analysis relying on the limited experimental information available to date. Decomposition reactions to solid precursors $PbX_2(s)$ and $CH_3NH_3X(s)$ are shown to be thermodynamically disfavored for X = Cl, Br, in great part because of the large negative decomposition entropies. For X = I, the serious discrepancy between the calorimetric determinations does not allow one to draw definitive conclusions on the thermodynamic driving force of this decomposition pathway, although the entropic contribution certainly also plays a large stabilizing role in this case. Decomposition reactions are most likely to occur by the release of gaseous products, a process that, according to recent experimental findings, may play an important role even in encapsulated devices. However, the identification of the molecular species lost by the perovskite structure is still uncertain, and the limited experimental information is not conclusive. Decomposition to $NH_3(g)$ and $CH_3X(g)$ is largely favored from a thermodynamic point of view, but it seems to suffer from a severe kinetic limitation related to the breaking of the strong C−N bond in the organic cation, as previously observed in the thermal decomposition of alkylammonium halides. Indeed, TGA-MS measurements support the occurrence of this decomposition channel at high temperature. However, effusion experiments indicate, in spite of thermodynamic driving forces, the release of $HX(g)$ and $CH_3NH_2(g)$, rather than $NH_3(g)$ and $CH_3X(g)$, at temperatures much lower than the decomposition temperatures detected by TGA experiments. The thermodynamic pathway becomes more important at higher temperature and under closer-to-equilibrium effusion conditions. The release of undissociated $CH_3NH_3X(g)$ molecules seems thermodynamically disfavored, although accurate thermodynamic data for these species are lacking. While thermodynamics prove to be very useful in rationalizing the degradation behavior of perovskite materials and corresponding precursors, careful attention has to paid to kinetic effects. However, the scarcity and the uncertainty of the experimental data currently available is a serious limit to thermodynamic predictions, which would greatly benefit from increased research efforts aimed at determining accurate thermodynamic information by independent techniques under various conditions. It is desirable that, in the next years, chemical thermodynamics research will give a greater contribution to assess the stability and the suitability of perovskite materials for photovoltaics and, more generally, to help the development of advanced materials for energy applications.[65]

AUTHOR INFORMATION

Corresponding Author

*E-mail: andrea.ciccioli@uniroma1.it.

ORCID

Andrea Ciccioli: 0000-0003-1421-8062

Alessandro Latini: 0000-0002-3205-4826

Notes

The authors declare no competing financial interest.

Biographies

Andrea Ciccioli (born 1969) is a Senior Scientist at the Department of Chemistry of the University of Rome "La Sapienza". His current research interests include the determination of thermodynamic properties of condensed phases by tensimetric measurements, the investigation of the evaporation/decomposition behavior of ionic liquids and hybrid materials, the experimental and computational study of bond energies of gaseous molecules.

Alessandro Latini was born in Rome, Italy, in 1974. He obtained a Master degree in Chemistry and a Ph.D. in Chemical Sciences (2006) from the University of Rome "La Sapienza", where he presently works as a Senior Scientist. His research is focused on the synthesis, characterization, and thermodynamic analysis of inorganic and hybrid materials, with special focus on advanced materials for energy conversion. He has coauthored 62 publications in international peer-reviewed journals.

ACKNOWLEDGMENTS

Authors wish to thank warmly Prof. Eric V. Patterson (Stony Brook University, New York, USA) for sharing unpublished computational results on the $CH_3NH_3I(g)$ dissociation reaction, and Prof. Rohan Mishra (Washington University in St. Louis, St. Louis, Missouri, USA) for providing numerical values of the theoretical decomposition enthalpies of $CH_3NH_3PbX_3$. The work done by Mr. Niccolò Iacovelli in preparing Figures 1, 2, 5, and the TOC/abstract graphic is gratefully acknowledged.

REFERENCES

(1) Asghar, M. I.; Zhang, J.; Wang, H.; Lund, P. D. Device Stability of perovskite Solar Cells: A review. *Renewable Sustainable Energy Rev.* **2017**, *77*, 131−146.

(2) Berhe, T. A.; Su, W.-N.; Chen, C.-H.; Pan, C.-J.; Cheng, J.-H.; Chen, H.-M.; Tsai, M.-C.; Chen, L.-Y.; Dubale, A. A.; Hwang, B.-J. Organometal Halide Perovskite Solar Cells: Degradation and Staility. *Energy Environ. Sci.* **2016**, *9*, 323−356.

(3) Manser, J. S.; Saidaminov, M. I.; Christians, J. A.; Bakr, O. M.; Kamat, P. V. Making and Breaking of Lead Halide Perovskites. *Acc. Chem. Res.* **2016**, *49*, 330−338.

DOI: 10.1021/acs.jpclett.8b00463
J. Phys. Chem. Lett. XXXX, XXX, XXX−XXX

(4) Wang, D.; Wright, M.; Elumalai, N. K.; Uddin, A. Stability of perovskite Solar Cells. Solar Energy Mater. *Sol. Energy Mater. Sol. Cells* **2016**, *147*, 255−275.
(5) Leijtens, T.; Eperon, G. E.; Noel, N. K.; Habisreutinger, S. N.; Petrozza, A.; Snaith, H. J. Stability of Metal Halide Perovskite Solar Cells. *Adv. Energy Mater.* **2015**, *5*, 1500963.
(6) Niu, G.; Guo, X.; Wang, L. Review of Recent Progress in Chemical Stability of Perovskite Solar Cells. *J. Mater. Chem. A* **2015**, *3*, 8970−8980.
(7) Ono, L. K.; Juarez-Perez, E. J.; Qi, Y. Progress on Perovskite Materials and Solar Cells with Mixed Cations and Halide Anions. *ACS Appl. Mater. Interfaces* **2017**, *9*, 30197−30246.
(8) Chen, J.; Cai, X.; Yang, D.; Song, D.; Wang, J.; Jiang, J.; Ma, A.; Lv, S.; Hu, M. Z.; Ni, C. Recent Progress in Stabilizing Hybrid Perovskites for Solar Cell Applications. *J. Power Sources* **2017**, *355*, 98−133.
(9) Slavney, A. H.; Smaha, R. W.; Smith, I. C.; Jaffe, A.; Umeyama, D.; Karunadasa, H. I. Chemical Approach to Addressing the Instability and Toxicity of Lead-Halide Perovskite Absorbers. *Inorg. Chem.* **2017**, *56*, 46−55.
(10) Ito, S.; Tanaka, S.; Manabe, K.; Nishino, H. Effects of Surface Blocking Layer of Sb_2S_3 on Nanocrystalline TiO_2 for $CH_3NH_3PbI_3$ Perovskite Solar Cells. *J. Phys. Chem. C* **2014**, *118*, 16995−17000.
(11) Matteocci, F.; Cinà, L.; Lamanna, E.; Cacovich, S.; Divitini, G.; Midgley, P. A.; Ducati, C.; Di Carlo, A. Encapsulation for Long-Term Stability Enhancement of Perovskite Solar Cells. *Nano Energy* **2016**, *30*, 162−172.
(12) Huang, J.; Tan, S.; Lund, P. D.; Zhou, H. Impact of H2O on Organic-Inorganic Hybrid Perovskite Solar Cells. *Energy Environ. Sci.* **2017**, *10*, 2284−2311.
(13) Matsumoto, F.; Vorpahl, S. M.; Banks, J. Q.; Sengupta, E.; Ginger, D. S. Photodecomposition and Morphology Evolution of Organometal Halide Perovskite Solar Cells. *J. Phys. Chem. C* **2015**, *119*, 20810−20816.
(14) Poorkazem, K.; Kelly, T. L. Compositional Engineering to Improve the Stability of Lead Halide Perovskites: A comparative Study of Cationic and Anionic Dopants. *ACS Appl. Energy Mater.* **2018**, *1*, 181−190.
(15) Ono, L. K.; Qi, Y. Surface and Interface Aspects of Organometal Halide Perovskite Materials and Solar Cells. *J. Phys. Chem. Lett.* **2016**, *7*, 4764−4794.
(16) Guerrero, A.; You, J.; Aranda, C.; Kang, Y. O.; Garcia-Belmonte, G.; Zhou, H.; Bisquert, J.; Yang, Y. Interfacial Degradation of Planar Lead Halide Perovskite Solar Cells. *ACS Nano* **2016**, *10*, 218−224.
(17) Huang, W.; Manser, J. S.; Kamat, P. V.; Ptasinska, S. Evolution of Chemical Composition, Morphology, and Photovoltaic Efficiency of $CH_3NH_3PbI_3$ Perovskite under Ambient Conditions. Chem. *Chem. Mater.* **2016**, *28*, 303−311.
(18) Koocher, N. Z.; Saldana-Greco, D.; Wang, F.; Liu, S.; Rappe, A. M. Polarization Dependenceof Water Adsoprtion to $CH_3NH_3PbI_3$ (001). *J. Phys. Chem. Lett.* **2015**, *6*, 4371−438.
(19) Yuan, H.; Debroye, E.; Janssen, K.; Naiki, H.; Steuwe, C.; Lu, G.; Moris, M.; Orgiu, E.; Uji-I, H.; De Schryver, F.; Samorì, P.; et al. Degradation of Methylammonium Lead Iodide Perovskite Structures through Light and Electron Beam Driven Ion Migration. *J. Phys. Chem. Lett.* **2016**, *7*, 561−566.
(20) Philippe, B.; Park, B.-W.; Lindblad, R.; Oscarsson, J.; Ahmadi, S.; Johansson, E. M.; Rensmo, H. Chemical and Electronic Structure Characterization of Led Halide Perovskite and Stabilityi Behavior under Different Exposures − A Photoelectron Spectroscopy Investigation. *Chem. Mater.* **2015**, *27*, 1720−1731.
(21) Akbulatov, A. F.; Luchkin, S. Yu.; Frolova, L. A.; Dremova, N. N.; Gerasimov, K. L.; Zhidkov, I. S.; Anokhin, A. V.; Kurmaev, E. Z.; Stevenson, K. J.; Troshin, P. A. Probing the Intrinsic Thermal and Photochemical Stability of Hybrid and Inorganic Lead Halide Perovskites. *J. Phys. Chem. Lett.* **2017**, *8*, 1211−1218.
(22) Conings, B.; Drijkoningen, J.; Gauquelin, N.; Babayigit, A.; D'Haen, J.; D'Olieslaeger, L.; Ethirajan, A.; Verbeeck, J.; Manca, J.; Mosconi, E.; De Angelis, F.; Boyen, H.-G. Intrinsic Thermal Instability of Methylammonium Lead Trihalide Perovskite. *Adv. Energy Mater.* **2015**, *5*, 1500477.
(23) Dualeh, A.; Gao, P.; Seok, S. I.; Nazeeruddin, M. K.; Grätzel, M. Thermal Behavior of Methyilammonium Lead-Trihalide Perovskite Photovoltaic Light Harvester. *Chem. Mater.* **2014**, *26*, 6160−6164.
(24) Alberti, A.; Deretzis, I.; Pellegrino, G.; Bongiorno, C.; Smecca, E.; Mannino, G.; Giannazzo, F.; Condorelli, G. G.; Sakai, N.; Miyasaka, T.; et al. Similar Structural Dynamics for the Degradation of $CH_3NH_3PbI_3$ in Air and in Vacuum. *ChemPhysChem* **2015**, *16*, 3064−3071.
(25) Ivanov, I. L.; Steparuk, A. S.; Bolyachkina, M. S.; Tsvetkov, D. S.; Safronov, A. P.; Zuev, A. Yu. Thermodynamics of formation of hybrid perovskite-type methylammonium lead halides. *J. Chem. Thermodyn.* **2018**, *116*, 253−258.
(26) Nagabhushana, G. P.; Shivaramaiah, R.; Navrotsky, A. Direct Calorimetric Verification of Thermodynamic Instability of Lead Halide Hybrid Perovskites. *Proc. Natl. Acad. Sci. U. S. A.* **2016**, *113*, 7717−7721.
(27) Brunetti, B.; Cavallo, C.; Ciccioli, A.; Gigli, G.; Latini, A. On the Thermal and Thermodynamic (In)stability of Methylammonium Lead Halide Perovskites. *Sci. Rep.* **2016**, *6*, 31896; Corrigendum: On the Thermal and Thermodynamic (In)Stability of Methylammonium Lead Halide Perovskites. *Sci. Rep* **2017**, *7*, 46867.
(28) Thind, A. S.; Huang, X.; Sun, J.; Mishra, R. First-Principle Prediction of a Stable Hexagonal Phase of $CH_3NH_3PbI_3$. *Chem. Mater.* **2017**, *29*, 6003−6011.
(29) Faghihnasiri, M.; Izadifard, M.; Ghazi, M. E. DFT Study of Mechanical Properties and Stability of Cubic Methylammonium Lead Halide Perovskites ($CH_3NH_3PbX_3$, X = I, Br, Cl). *J. Phys. Chem. C* **2017**, *121*, 27059−27070.
(30) Yang, D.; Lv, J.; Zhao, X.; Xu, Q.; Fu, Y.; Zhan, F.; Zunger, A.; Zhang, L. Functionality-Directed Screening of Pb-Free Hybrid Organic-Inorganic Perovskites with Desired Intrinsic Photovoltaic Functionalities. *Chem. Mater.* **2017**, *29*, 524−538.
(31) Buin, A.; Comin, R.; Xu, J.; Ip, A. H.; Sargent, E. H. Halide-Dependent Electronic Structure of Organolead Perovskite Materials. *Chem. Mater.* **2015**, *27*, 4405−4412.
(32) Zhang, Y.-Y.; Chen, S.; Xu, P.; Xiang, H.; Gong, X.-G.; Walsh, A.; Wei, S.-H. Intrinsic Instability of the Hybrid Halide Perovskite Semiconductor $CH_3NH_3PbI_3$. *arXiv.org, e-Print Arch., Condens. Matter* **2015**, No. arXiv:1506.01301.
(33) Buin, A.; Pietsch, P.; Xu, J.; Voznyy, O.; Ip, A. H.; Comin, R.; Sargent, E. H. Materials Processing Routes to Trap-Free Halide Perovskites. *Nano Lett.* **2014**, *14*, 6281−6286.
(34) Tenuta, E.; Zheng, C.; Rubel, O. Thermodynamic Origin of Instability in Hybrid Halide Perovskites. *Sci. Rep.* **2016**, *6*, 37654.
(35) Ganose, A. M.; Savory, C. N.; Scanlon, D. O. $(CH_3NH_3)_2Pb(SCN)_2I_2$: A More Stable Structural Motif for Hybrid Halide Photovoltaics ? *J. Phys. Chem. Lett.* **2015**, *6*, 4594−4598.
(36) Zheng, C.; Rubel, O. Ionization Energy as a Stability Criterion for Halide Perovskites. *J. Phys. Chem. C* **2017**, *121*, 11977−11984.
(37) Yang, B.; Dyck, O.; Ming, W.; Du, M.-H.; Das, S.; Rouleau, C. M.; Duscher, G.; Geohegan, D. B.; Xiao, K. Observation of Nanoscale Morphological and Structural Degradation in Perovskite Solar Cells by in Situ TEM. *ACS Appl. Mater. Interfaces* **2016**, *8*, 32333−32340.
(38) Agiorgousis, M. L.; Sun, Y.-Y.; Zeng, A.; Zhang, S. Strong Covalency-Induced Recombination Centers in Perovskite Solar Cell Material $CH_3NH_3PbI_3$. *J. Am. Chem. Soc.* **2014**, *136*, 14570−14575.
(39) Haruyama, J.; Sodeyama, K.; Han, L.; Tateyama, Y. Termination Dependence of Tetragonal $CH_3NH_3PbI_3$ Surfaces for Perovskite Solar Cells. *J. Phys. Chem. Lett.* **2014**, *5*, 2903−2909.
(40) Yin, W.- J.; Shi, T.; Yan, Y. Unusual Defect Physics in $CH_3NH_3PbI_3$ Perovskite Solar Cell Absorbers. *Appl. Phys. Lett.* **2014**, *104*, 063903.
(41) Onoda-Yamamuro, N.; Matsuo, T.; Suga, H. Calorimetric and IR Spectroscopic Studies of Phase Transitions in Methylammonium

DOI: 10.1021/acs.jpclett.8b00463
J. Phys. Chem. Lett. XXXX, XXX, XXX−XXX

Trihalogenoplumbates (II). *J. Phys. Chem. Solids* **1990**, *51*, 1383–1395.
(42) Glasser, L.; Jenkins, D. D. B. Standard Absolute Entropies, S°_{298}, from Volume or Density. Part II. Organic Liquids and Solids. *Thermochim. Acta* **2004**, *414*, 125–130.
(43) El-Mellouhi, F.; Bentria, E. T.; Rashkeev, S. N.; Kais, S.; Alharbi, F. H. Enhancing Intrinsic Stability of Hybrid Perovskite Sola Cell by Strong, yet Balanced, Electronic Coupling. *Sci. Rep.* **2016**, *6*, 30305.
(44) Chun-Ren Ke, J.; Walton, A. S.; Lewis, D. J.; Tedstone, A.; O'Brien, P.; Thomas, A. G.; Flavell, W. R. In situ Investigation of Degradation at Organometal Halide Perovskite Surfaces by X-Ray Photoeectron Spectroscopy at Realistic Water Vapour Pressure. *Chem. Commun.* **2017**, *53*, 5231.
(45) Hong, F.; Saparov, B.; Meng, W.; Xiao, Z.; Mitzi, D. B.; Yan, Y. Viability of Lead-Free Perovskites with Mixed Chalcogen and Halogen Anions for Photovoltaic Applications. *J. Phys. Chem. C* **2016**, *120*, 6435–6441.
(46) Kim, N.-K.; Min, Y. H.; Noh, S.; Cho, E.; Jeong, G.; Joo, M.; Ahn, S.-W.; Lee, J. S.; Kim, S.; Ihm, K.; Ahn, H.; et al. Investigation of Thermally Induced Degradation in $CH_3NH_3PbI_3$ Perovskite Solar Cells Using In-situ Synchrotron Radiation Analysis. *Sci. Rep.* **2017**, *7*, 4645.
(47) Song, Z.; Watthage, S. C.; Phillips, A. B.; Tompkins, B. L.; Ellingson, R. J.; Heben, M. J. Impact of Processing Temperature and Composition on the Formation of Methylammonium Lead Iodide Perovskites. *Chem. Mater.* **2015**, *27*, 4612–4619.
(48) Leyden, M. R.; Meng, L.; Jiang, Y.; Ono, L. K.; Qiu, L.; Juarez-Perez, E. J.; Qin, C.; Adachi, C.; Qi, Y. Methylammonium Lead Bromide Perovskite Light-Emitting Diodes by Chemical Vapor deposition. *J. Phys. Chem. Lett.* **2017**, *8*, 3193–3198.
(49) Juarez-Perez, E. J.; Hawash, Z.; Raga, S. R.; Ono, L. K.; Qi, Y. Thermal Degradation of $CH_3NH_3PbI_3$ Perovskite into NH_3 and CH_3I Gases Observed by Coupled Thermogravimetry-Mass Spectrometry Analysis. *Energy Environ. Sci.* **2016**, *9*, 3406–3410.
(50) Latini, A.; Gigli, G.; Ciccioli, A. A Study on the Nature of the Thermal Decomposition of Methylammonium Lead Iodide Perovskite $CH_3NH_3PbI_3$: An attempt to Rationalise Contradictory Experimental Results. *Sustainable Energy Fuels* **2017**, *1*, 1351.
(51) Deretzis, I.; Alberti, A.; Pellegrino, G.; Smecca, E.; Giannazzo, F.; Sakai, N.; Miyasaka, T.; LaMagna, A. Atomistic Origins of $CH_3NH_3PbI_3$ degradation to PbI_2 in vacuum. *Appl. Phys. Lett.* **2015**, *106*, 131904.
(52) Stoumpos, C. C.; Malliakas, C. D.; Kanatzidis, M. G. Semiconducting Tin and Lead Iodide Perovskites with Organic Cations: Phase Transitions, High Mobilities, and Near-Infrared Photoluminescent Properties. *Inorg. Chem.* **2013**, *52*, 9019–9038.
(53) Dimesso, L.; Dimamay, M.; Hamburger, M.; Jaegermann, W. Properties of CH3NH3PbX3 (X = I, Br, Cl) Powders as Precursors for Organic/Inorganic Solar Cells. *Chem. Mater.* **2014**, *26*, 6762–6770.
(54) Nenon, D. P.; Christians, J. A.; Wheeler, L. M.; Blackburn, J. L.; Sanehira, E. M.; Dou, B.; Olsen, M. L.; Zhu, K.; Berry, J. J.; Luther, J. M. Structural and Chemical Evolution of Methylammonium Lead Halide Perovskites During Thermal Processing from Solution. *Energy Environ. Sci.* **2016**, *9*, 2072–2082.
(55) Kottokkaran, R.; Abbas, H.; Balaji, G.; Zhang, L.; Samiee, M.; Kitahara, A.; Noack, M.; Dalal, V. Highly Reproducible Vapor Deposition Technique, Device Physics and Structural Instability of Perovskite Solar Cells. *IEEE 42nd Photovoltaic Specialist Conference (PVSC)* **2015**, *42*, 1–4.
(56) Williams, A. E.; Holliman, P. J.; Carnie, M. J.; Davies, M. L.; Worsley, D. A.; Watson, T. M. Perovskite Processing for Photovoltaics: A Spectrothermal Evaluation. *J. Mater. Chem. A* **2014**, *2*, 19338–19346.
(57) Showman, A. P. Hydrogen Halides on Jupiter and Saturn. *Icarus* **2001**, *152*, 140–150.
(58) Jay, A. N.; Daniel, K. A.; Patterson, E. V. Atom-Centered Density Matrix Propagation Calculations on the Methyl Transfer from CH_3Cl to NH_3: Gas-Phase and Continuum-Solvated Trajectories. *J. Chem. Theory Comput.* **2007**, *3*, 336–343.
(59) Patterson, E. V. Private communication.
(60) Note that, while the derivation of total pressure from KEML measurements requires the gas phase composition to be known, assuming the occurrence of processes 8, 9, or 10 has a very small effect on the calculated pressure, because the relevant average molecular mass of the vapor phase is very similar in all three cases (see ref 27).
(61) Łubkowski, J.; Błażejowski, J. Thermal Properties and Thermochemistry of Alkanaminium Bromides. *Thermochim. Acta* **1990**, *157*, 259–277.
(62) Dokurno, P.; Łubkowski, J.; Błażejowski, J. Thermal Properties, Thermolysis and Thermochemistry of Alkanaminium Iodides. *Thermochim. Acta* **1990**, *165*, 31–48.
(63) Sawicka, M.; Storoniak, P.; Skurski, P.; Błażejowski, J.; Rak, J. TG-FTIR, DSC and Quantum Chemical Studies of the Thermal Decomposition of Quaternary Methylammonium Halides. *Chem. Phys.* **2006**, *324*, 425–437.
(64) Dong, C.; Song, X.; Meijer, E. J.; Chen, G.; Xu, Y.; Yu, J. Mechanism Studies on Thermal Dissociation of tri-*n*-octylamine hydrochloride with FTIR, TG, DSC and quantum chemical methods. *J. Chem. Sci.* **2017**, *129*, 1431–1440.
(65) https://www.thermocon.org/.

DOI: 10.1021/acs.jpclett.8b00463
J. Phys. Chem. Lett. XXXX, XXX, XXX–XXX